Journal of Paleolimnology **30:** 307–320, 2003.
© 2003 *Kluwer Academic Publishers. Printed in the Netherlands.*

9000 years of geochemical evolution of lithogenic major and trace elements in the sediment of an alpine lake – the role of climate, vegetation, and land-use history

Karin A. Koinig[1]*, William Shotyk[1], André F. Lotter[2,3], Christian Ohlendorf[4] and Michael Sturm[4]
[1]*Institute of Geology, University of Bern, Baltzerstrasse 1, CH-3012 Bern, Switzerland*
[2]*Geobotanical Institute, University of Bern, Altenbergrain 21, CH-3013 Bern, Switzerland*
[3]*University of Utrecht, Laboratory of Palaeobotany and Palynology, Budapestlaan 4, 3584 CD Utrecht, The Netherlands*
[4]*Swiss Federal Institute of Environmental Science and Technology (EAWAG), Überlandstrasse 33, CH-8600 Dübendorf, Switzerland*
Present addresses: K.A. Koinig, Institute of Zoology and Limnology, University of Innsbruck, Technikerstr. 25, A-6020 Innsbruck, Austria W. Shotyk, Institute of Environmental Geochemistry, University of Heidelberg, Im Neuenheimer Feld 236, D-69120 Heidelberg, Germany
**Author for correspondence (E-mail: karin.koinig@uibk.ac.at)*

Received 23 January 2001; accepted 24 March 2003

Key words: Sediment geochemistry, Trace-metals, Weathering, Erosion, Manganese, Carbonate, Anoxia

Abstract

A 9000 cal. year record of geochemistry was analysed in a sediment core obtained from a Swiss alpine hard-water lake (1937 m a.s.l.) that is located at the present-day tree-line. Geochemical stratigraphies are compared to changes in mineralogy, grain-size, pollen, and macrofossil records. This allows the reconstruction of the effects of changes in vegetation and of 3500 years of land-use in the catchment area on sediment geochemistry. Using principal component analysis, two major geochemical groups are distinguished: (i) Changes in concentrations of Rb, Ti, Zr, Fe, As, and Pb are closely related to corresponding changes in the concentrations of quartz and clay. They are thus considered to represent the silicate fraction which shows an increase from the oldest to the youngest core section. (ii) In contrast, Ca and Sr concentrations are positively correlated with changes in silt, sand, and calcite. They are therefore considered to represent the carbonate fraction which gradually decreased. Based on constrained cluster analysis, the core is divided into two major zones. The oldest zone (A; 9000–6400 cal. BP) is characterised by high concentrations of detrital carbonates. The more open catchment vegetation at that time promoted the physical weathering of these carbonates. The second major zone (B, 6400 cal. BP–1996 AD) is divided into four subsections with boundaries at ca. 3500, 2400, and 160 cal. BP. The lower part of this zone, B1, is characterized by a gradual decrease in the carbonate-silt fraction and a pronounced increase in the silicate-clay fraction. This is concurrent with the expansion of *Picea* in the catchment area, which probably stabilized the soil. The middle part, B2 and B3 (3500–160 cal. BP), comprises pronounced fluctuations in all elements, especially Ca, Sr, Mn, and Rb, but also in clay and silt. These changes are related to varying intensities of alpine farming. In the same section, Mn/Fe ratios are highly variable, suggesting changes in the mixing regime of the lake with phases of anoxic bottom water. The uppermost section, B4 (since 160 cal. BP), is characterized by a steep decline in the silicate fraction and an increase in Ca and Sr. Despite the decrease in the silicate fraction, Pb increases, due to elevated atmospheric input resulting from early metal pollution, are masked by the high natural variability. Generally, changes in vegetation, which correspond to climate changes in the early Holocene and to human activities since ca. 3700 cal. BP, are the controlling factor for variations in the geochemical composition of the sediment of Sägistalsee.

This is the sixth in a series of eight papers published in this special issue dedicated to the palaeolimnology of Sägistalsee. Drs. André F. Lotter and H. John B. Birks were the guest editors of this issue.

source: https://doi.org/10.7892/boris.135410 | downloaded: 16.5.2021

Introduction

Lake sediments allow the study of long-term natural environmental variations and of the impact of early and recent human activities on lakes and their catchments. Most studies performed on freshwater lake sediments have focused on changes in biological proxies. Apart from saline lakes, few studies have analysed long-term changes in sediment geochemistry in detail (e.g., Norton and Kahl, 1991; Norton et al., 1992; Kauppila and Salonen, 1997; Wolfe and Hartling, 1997). More commonly, investigations have focused on trace-metal trends as indicators of atmospheric pollution (e.g., Blais and Kalff, 1993; Renberg et al., 1994; Camarero et al., 1998; Brännvall et al., 1999) or on changes in carbonates as indicators of climate or trophic change (e.g., Wessels et al., 1995; Dean, 1999). Several studies also present changes in stable isotopes as indicators of changes in climate, salinity, or trophic state (e.g., Valero-Garces et al., 1997; Brenner et al., 1999; Lamb et al., 1999; Schwalb et al., 1999, Teranes et al., 1999). However, special types of XRF-analyses of bulk geochemistry offer a fast and inexpensive tool to quantify lithogenic elements such as Ti, Zr, Rb, Sr, Fe, and Mn, and also Pb, As, Zn, Cu, and Cr (Cheburkin and Shotyk, 1996; Cheburkin et al., 1997; Boyle, 2000). These can provide insights into the causes, timing and extent of changes in the weathering regime of the catchment. Furthermore, these analyses allow detection of changes in atmospheric deposition (e.g., Pb pollution or soil dust) and in redox conditions (Mn/Fe ratio).

Among the long-term palaeoenvironmental changes reflected in sediment geochemistry, the impact of climate is of major interest. Climatic variations affect the transport of lithogenic elements from the catchment to a lake. During warm periods, chemical weathering might be accelerated (e.g., Sommaruga-Wögrath et al., 1997; White et al., 1999), while the denser vegetation cover and more stable soils may reduce physical weathering (e.g., Kauppila and Salonen, 1997). In contrast, physical weathering is elevated during cold periods when vegetation cover is reduced and higher amounts of dust are transported to the lake. Also various human impacts can be traced in sediment geochemistry. Deforestation and agriculture influence soil stabilisation and erosion (e.g., Wilmshurst, 1997). Anthropogenic atmospheric deposition affects trace-metal concentrations (e.g., Brännvall et al., 2001). Land-use affects nutrient concentrations and the redox and mixing regimes of lakes (e.g., Engstrom et al., 1985; Lotter, 2000). In consequence, many changes in sediment geochemistry may be observed.

Here we investigate the changes in lithogenic major and trace elements in an alpine hard-water lake and assess their value as indicators for natural and anthropogenic changes in the catchment. We address the following questions: (1) What is the impact of climate change on bulk sediment geochemistry? Is it mainly a direct (weathering, in-lake processes) or an indirect (vegetation, soil development) influence that we observe in the sediment? (2) How did early human activities in the catchment area (e.g., the onset and development of alpine pasturing) affect sediment geochemistry? (3) Is it possible to detect signals of early anthropogenic atmospheric metal deposition?

Study area

Sägistalsee (46°40′50″N, 7°58′40″E) is located in the Bernese Alps, Switzerland, at 1935 m a.s.l. It has a water surface area of 0.073 km², a volume of 490,600 m³, and a maximum depth of 9.7 m. The extent of the watershed is 4.12 km². The lake is fed by 4 surface inflows and has one subsurface outflow. The lake is a mesotrophic (total phosphorus 20 µg l^{-1}, total nitrogen 0.39 mg l^{-1}, DOC 0.9 mg C l^{-1}), alpine hard-water lake (pH 8.4; alkalinity 2.7 meq l^{-1}; 52 mg Ca l^{-1}) with a conductivity of 225 µS cm^{-1}. The catchment mainly consists of calcareous bedrock. The steep slopes are composed of black and yellow-brown limestone which are partly found as breccia with siderolithic weathering crusts and which contain some oolithic ironstone. The flatter basement consists of carbonaceous, clay-rich Vallanginien schist and dark marl. Located at present-day tree-line, the lake is expected to be sensitive to climate-driven changes in vegetation. Lotter and Birks (2003) give a more detailed description of the lake and catchment characteristics.

Materials and methods

A 13.5 m long core was retrieved from Sägistalsee in 1996 using a Livingstone piston corer. For analyses of the top 50 cm, a short sediment core was retrieved with a gravity corer. The core was subsampled in 1 or 2 cm slices for different analyses including pollen and plant macrofossils (Wick et al., 2003), chironomids (Heiri and Lotter, 2003), cladocera (Hofmann, 2003), grain-size, mineralogy, organic and inorganic carbon (Ohlendorf et al., 2003), and inorganic geochemistry.

A total of 176 sub-samples (1–2 cm thick, on average at 6–8 cm intervals corresponding to an average time interval of 47 yrs) have been analysed for bulk geochemistry. The samples were dried at 105 °C and ground with an agate ball mill. Selected major and trace elements (As, Ca, Cr, Cu, Fe, K, Mn, Ni, Pb, Rb, Sr, Ti, Zn, and Zr) were analysed with an energy-dispersive miniprobe multi-element analyser (EMMA), a special type of X-ray fluorescence analyser consisting of a conventional X-ray tube with Mo target (17.44 keV, Mo Kα), a focused LiF (220) variable wavelength monochromator, and a rotating sample holder. Detection is accomplished with a Si(Li) detector (for detailed description of EMMA see Cheburkin and Shotyk, 1996; Cheburkin et al., 1997). From each sample, about 0.8–1.5 g dried sediment were analysed as loose powder without further treatment. Lower limits of detection for the elements are given in Table 1. Due to the inherent limitations of the EMMA instrument, Ca and K measurements are subject to relatively high standard errors (15% for Ca, 20% for K; based on the analyses of 12 standard reference materials consisting either of sediment, soil, or coal fly-ash). Thus Sr and Rb profiles were used for comparison with grain-size and mineralogy. In addition, high iron concentrations increase the analytical errors for Mn and Ti (and also K and Ca) because of the higher absorption of their characteristic X-rays in the sample. Ti is also affected by escape peaks from Fe-Kα and Fe-Kβ, which are located in the Ti-Kα region if the Fe concentration is high.

For trace-metals, which may be affected by recent anthropogenic activities such as Pb, As, and Zn, enrichment factors (EF) were calculated by normalizing the element/Zr ratio in the samples to the average element/Zr ratio in the section older than 6440 cal BP (= normalized, pre-anthropogenic background concentration of core zone A; see Equation 1). Zirconium (Zr) was used for normalization because it is a largely insoluble, immobile, and weathering-resistant element that is not utilized biologically and that has no significant anthropogenic sources. Thus Zr is widely used in weathering studies as a conservative lithogenic element against which elemental enrichments and depletions may be viewed. Subsequently, normalised concentrations and enrichment factors were used to separate natural, lithogenic inputs from anthropogenic ones.

$$EF = \frac{\left(\frac{metal}{Zr}\right)_{sample}}{\left(\frac{metal}{Zr}\right)_{background}} \quad (1)$$

Total carbon ($C_{tot.}$) was analysed using a CNS analyser (Carlo Erba). Inorganic carbon ($C_{inorg.}$) was measured as $CaCO_3$ with a Coulometer. Organic carbon ($C_{org.}$) was calculated as the difference between $C_{tot.}$ and $C_{inorg.}$ For analyses of mineralogy, bulk smear slides have been analysed with X-ray diffraction (XRD). XRD results are given as % peak-sum. To avoid confusion, we use $calcite_{coulom.}$ for calcite measured with the coulometer and $calcite_{XRD}$ for results from XRD analyses. Grain-size was determined on untreated sediments using a Laser-Particle-Analyser (Mastersizer). For details, see Ohlendorf et al. (2003).

Age dates are based on ^{14}C dates (AMS) of plant material from 17 samples. The model used for calculation of calibrated years is discussed in detail in Lotter and

Table 1. Range of concentrations measured for geochemical elements, lower limits of detection (LLD) and analytical errors

Element		Min	Max	Mean All	Mean Zone A	Mean Zone B	LLD	Analytical error (%)
Ca	[%]	8.81	27.21	17.17	15.42	20.63	0.1	15
Fe	[%]	2.50	6.49	3.31	3.51	2.91	0.01	10
K	[%]	2.94	8.52	4.22	4.57	3.52	0.1	20
Ti	[%]	0.33	0.91	0.45	0.48	0.38	0.01	10
As	[μg g^{-1}]	7	23	13	14	10	2	12
Mn	[μg g^{-1}]	277	1923	519	602	354	40	10
Pb	[μg g^{-1}]	14	47	21	23	17	1.8	7
Rb	[μg g^{-1}]	78	190	128	143	99	0.5	5
Sr	[μg g^{-1}]	308	531	427	396	488	0.7	7
Zn	[μg g^{-1}]	72	204	106	118	84	1.5	10
Zr	[μg g^{-1}]	113	213	150	160	129	1	10
Mn/Fe		0.028	0.192	0.052	0.060	0.035		

Birks (2003). The dates mentioned in this article refer to calibrated radiocarbon years before present (cal. BP) where 0 year is equal to 1950 AD.

All stratigraphies are depicted as running means (n = 5). Zonation is based on stratigraphically constrained cluster analyses calculated with ZONE (version 1.2 by Steve Juggins) first using only geochemical data (n = 176) and then including other data measured in the same horizon for comparison ($C_{inorg.}$ and $C_{org.}$, n = 169; + mineralogy data and grain-size fractions, n = 86). The number of statistical significant zones was determined for the results of an optimal sum-of-squares partition by comparison with the broken stick model (Bennett, 1996). For cluster analyses, data were ranged (Legendre and Legendre, 1998, p. 37) prior to analyses to allow for comparison of data measured in different units. Principal component analysis (PCA) and redundancy analysis (RDA) were performed on centred and standardized data using CANOCO for Windows 4.0 (ter Braak and Smilauer, 1998).

Results

General changes in lithogenic major and trace elements

Two contrasting trends are observed in the sediment geochemistry. While Sr and Ca concentrations (Fig. 1a) gradually decrease from the bottom to the top of the core, all other elements increase: Rb, K, Zr, Ti (Figs. 1b and 1c); Fe, Mn (Fig. 2); and Pb, As, Zn (Fig. 3). However, fluctuations are high for all elements, especially in sections B2, B3, and B4.

Based on the constrained cluster analysis results, the geochemical stratigraphies are split into seven signifi-

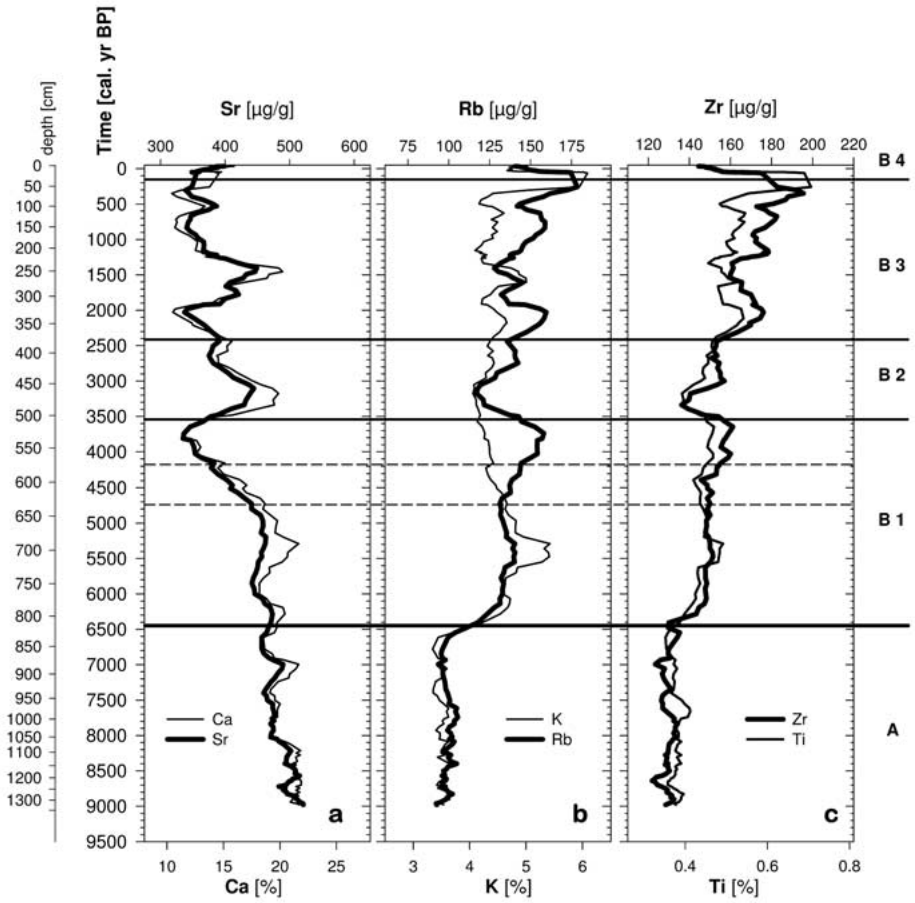

Fig. 1. Stratigraphies of lithogenic elements in Sägistalsee – concentrations of indicators for carbonate and silicate weathering: (a) strontium and calcium, (b) rubidium and potassium, (c) zircon and titanium. All concentrations are depicted as running means (n = 5).

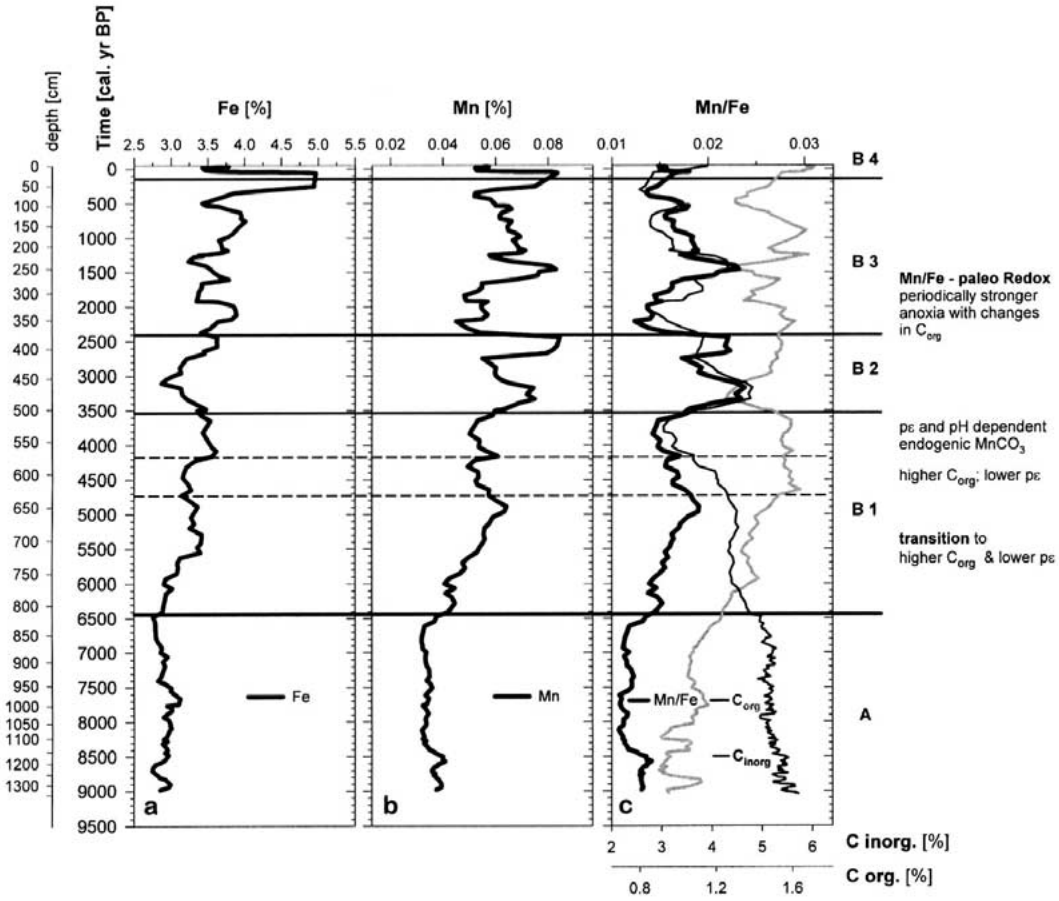

Fig. 2. Stratigraphies for concentrations of redox and pH-sensitive elements and for carbon in Sägistalsee: (a) iron, (b) manganese, (c) manganese to iron ratio (Mn/Fe, thick black line), C_{inorg} (measured as $calcite_{coulom}$, thin black line) and organic carbon (C_{org}, grey line). Major processes affecting Mn/Fe are mentioned on the right margin. All concentrations are depicted as running means (n = 5).

cant sections, which fall into two main zones. Zone A (9050–6440 cal. BP) is characterized by the highest levels of Sr and Ca observed in the core and by the lowest concentrations of all other elements. Sr and Ca (and also $calcite_{XRD}$ and $calcite_{coulom.}$) concentrations decrease slightly. All other elements show some fluctuations but remain within a constant range. Sediment accumulation rates are highest in the bottom of this section, reaching 0.33 cm yr^{-1} around 9050 cal. BP, but decreasing strongly to 0.20 cm yr^{-1} around 7900 cal. BP and to 0.11 cm yr^{-1} around 6440 cal. BP.

In zone B (6440 cal. BP–present), Ca and Sr concentrations (Fig. 1a) continue to decrease while all other elements start to increase (Figs 1b, 1c, 2 and 3). Three subsections are distinguished: In section B1 (6440–3540 cal. BP), the decline of Sr and Ca and the increase of many other elements are most distinct. Most pronounced increases are observed in Rb, while K increases only until ca. 5300 cal. BP and then starts to decrease (Fig. 1b). Concentrations of Pb (Fig. 3a) increase only slightly. As and Zn (Figs 3b and 3c) show a distinct increase between 6600 and 5700 cal. BP and then remain more or less stable. Sediment accumulation rates are lowest in this section, ranging between 0.11 cm yr^{-1} and 0.10 cm yr^{-1}. In sections B3 (3540–2410 cal. BP) and B2 (2410–160 cal. BP) variations are high for all elements. Generally Rb, Zr, Ti, Fe, Mn, Pb, As, and Zn are enriched, especially in section B2, and most elements (except Pb) reach their maximum at the top of this section. Sediment accumulation rate increases again from 0.10 cm yr^{-1} around 3540 cal. BP to 0.18 cm yr^{-1} around 500 cal. BP. Section B4 reflects the changes over the last 200 years. Here a reversal in trend is observed: concentrations of all elements show a steep decline

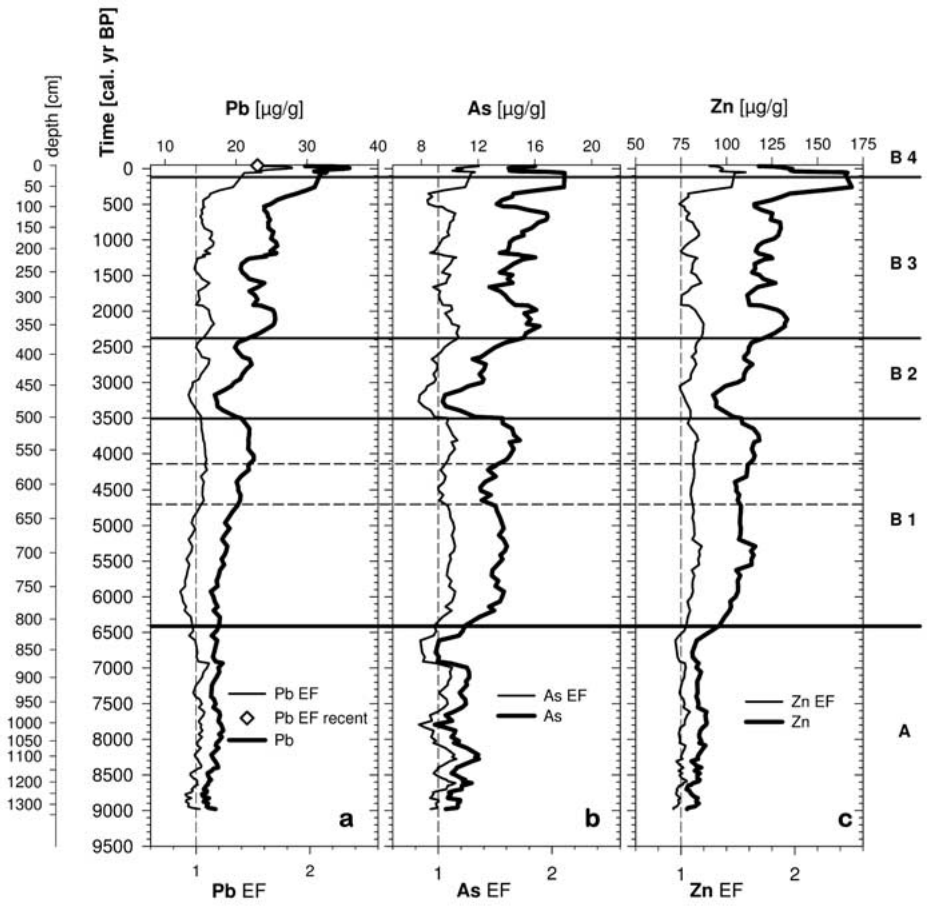

Fig. 3. Stratigraphies for concentrations and enrichment factors (EF) of trace-metals in Sägistalsee: (a) lead, (b) arsenic, and (c) zinc. All concentrations and EF are depicted as running means (n = 5). EF is calculated relative to Zr/metal ratios in section A.

except for Sr, Ca, and also Pb. The most remarkable feature of zone B is the synchronous changes in Mn, Mn/Fe, $C_{inorg.}$, Ca, and Sr since ca. 4000 cal. BP.

PCA of geochemistry, carbon, mineralogy, and grain-size data

In order to explain the high variability in lithogenic major and trace elements, statistical analyses were performed including (a) all geochemical parameters including $C_{inorg.}$, (b) grain-size, (c) mineralogy ($quartz_{XRD}$, $calcite_{XRD}$), and (d) organic parameters ($C_{org.}$). Using PCA, 72% of the variance within these data can be explained by the first two principal components (Fig. 4). An additional 10% is explained by component 3, and 5% by component 4. PCA axis 1 is positively correlated with $C_{inorg.}$ (r = 0.95) > Sr (0.88) > $calcite_{XRD}$ > coarse silt > medium grain-size > Ca > sand (r = 0.76) and also medium silt. In contrast, PCA axis one is negatively related to Rb (r = –0.98) > Zn > $C_{org.}$ > clay > fine silt > Ti > Zr > quartz > Pb > Fe (r = –0.72) and also As, K, Mn, and Mn/Fe. PCA axis 2 is mainly related to K (0.63), Mn (0.62), and Mn/Fe (0.60).

Of all the geochemical elements, the loadings of Rb and Sr on PCA axis 1 are highest. Their arrows point in opposite directions. Axis 1 thus reflects a gradient from Ca (and carbonate) rich samples to Rb (and clay) rich samples. Performing a RDA with Sr as the sole response data and manual forward selection in order to test which variables explain the highest proportion of the variation in Sr, $C_{inorg.}$ is chosen as the first predictor variable explaining 89% ($p < 0.001$) of the changes. Positive Sr correlations are strongest with Ca (r = 0.94, $p < 0.001$), $C_{inorg.}$ (r = 0.93, $p < 0.001$), and $calcite_{XRD}$ (r = 0.86, $p < 0.001$). This indicates that the sedimentation of Sr is strongly linked to that of $CaCO_3$ in this

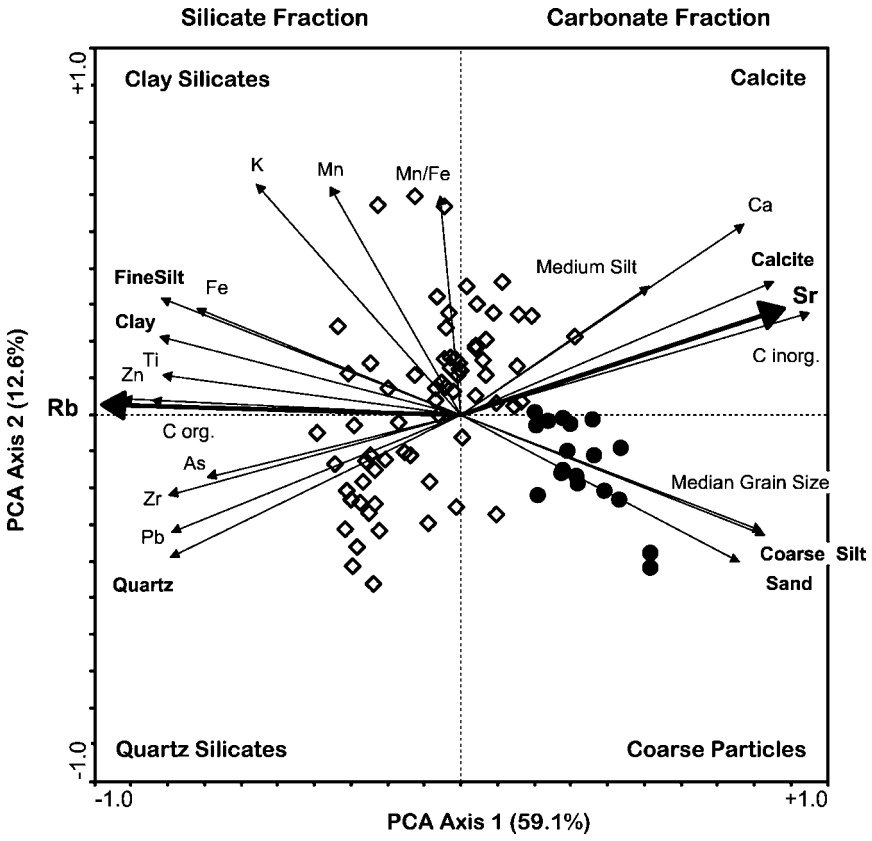

Fig. 4. Biplot based on principal component analyses of concentrations of lithogenic elements, organic and inorganic carbon, minerals, and grain-size fractions measured in the same sample horizons (n = 86). In order to depict the changes between zones A and B, the samples of each zone are marked differently: Black dots are samples of section A. Open diamonds are samples of section B.

lake, a finding which is generally expected as Sr is an abundant trace element in $CaCO_3$, especially when no aragonites are present, as is the case in these sediments. Rb is significantly positively correlated with all other geochemical elements, except Mn/Fe. Its variation is significantly negatively related to changes in $C_{inorg.}$ (first variable selected in RDA, 82%, $p < 0.001$), suggesting that it is bound mainly in the silicate fraction. A relative increase in the carbonate fraction will consequently cause a decrease in the silicate fraction and vice versa.

Based on these results, two major geochemical groups are distinguished (Fig. 4): (i) A carbonate fraction: Ca and Sr concentrations correlate with those of $calcite_{XRD}$, $C_{inorg.}$ (measured as $calcite_{coulom.}$), medium silt, coarse silt, and sand and can therefore be considered to represent the carbonate fraction. (ii) A silicate fraction: The changes in concentrations of Rb, Ti, Zr, Fe, Pb, As, Zn, Ni, and Cr, are closely related to corresponding changes in the concentrations of quartz, clay, and fine silt and can thus be considered to represent the silicate fraction. The changes between zones A and B are depicted in Fig. 4. The samples measured in zone A are all located in the carbonate-rich fraction, whereas there is a shift towards the silicate fraction with a higher proportion of fine grained particles in zone B.

Comparison of changes in sediment geochemistry with mineralogy and grain-size

For comparison of sediment geochemistry with the changes in mineralogical composition and grain-size fractions, we choose Rb as representative for the silicate fraction and Sr as representative for the carbonate fraction. These elements were selected because of their high loadings on PCA axis 1 and their contrasting trends. In addition, Rb and Sr probably reflect changes in the sediment sources with Rb mainly originating from clay-rich schist and marl, which form the catchment basement while the major source for Sr are the steep limestone slopes.

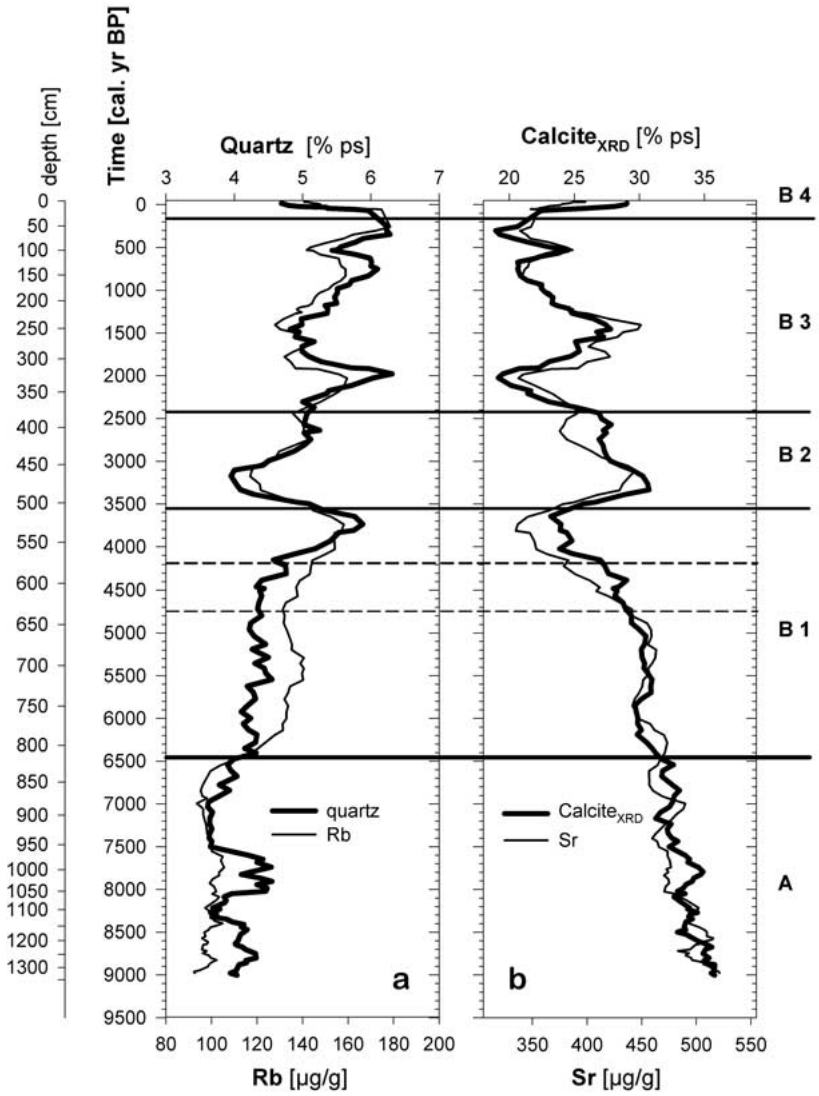

Fig. 5. Comparison of (a) rubidium concentrations and quartz (percent peak-sum), and (b) strontium concentrations and calcite$_{XRD}$ (percent peak-sum) in the sediment of Sägistalsee. All concentrations are depicted as running means (n = 5).

Figure 5 depicts the strong relationship between changes in mineralogical composition and sediment geochemistry: Rb follows the trend of quartz (Fig. 5a) while Sr follows calcite$_{XRD}$ (Fig. 5b). The trends are very similar throughout the whole core.

Rb and Sr stratigraphies are additionally compared with changes in grain-size (Fig. 6). As indicated by the PCA (Fig. 4), the Rb trends compare well with changes in the grain-size fraction smaller than 10 µm (i.e., fine silt and clay) throughout the core (Pearson $r = 0.86$, $p < 0.001$). The Sr concentration follows the trends of coarse particles (grain-size > 10 µm; Fig. 6b, $r = 0.71$, $p < 0.001$) and median grain-size ($r = 0.67$, $p < 0.001$). However, the depletion of coarse particles in the lower part of section B1 (6500–4700 cal. BP) is stronger than that of Sr (or Ca). The geochemistry is nevertheless strongly reflecting changes in grain-size. These changes are most likely related to changes in physical erosion. In Fig. 6, processes affecting erosion as a result of changes in vegetation cover and soil stabilisation are indicated. As discussed in more detail below, major shifts in sediment geochemistry are concurrent with changes in local vegetation as observed in the macrofossil records (Wick et al., 2003).

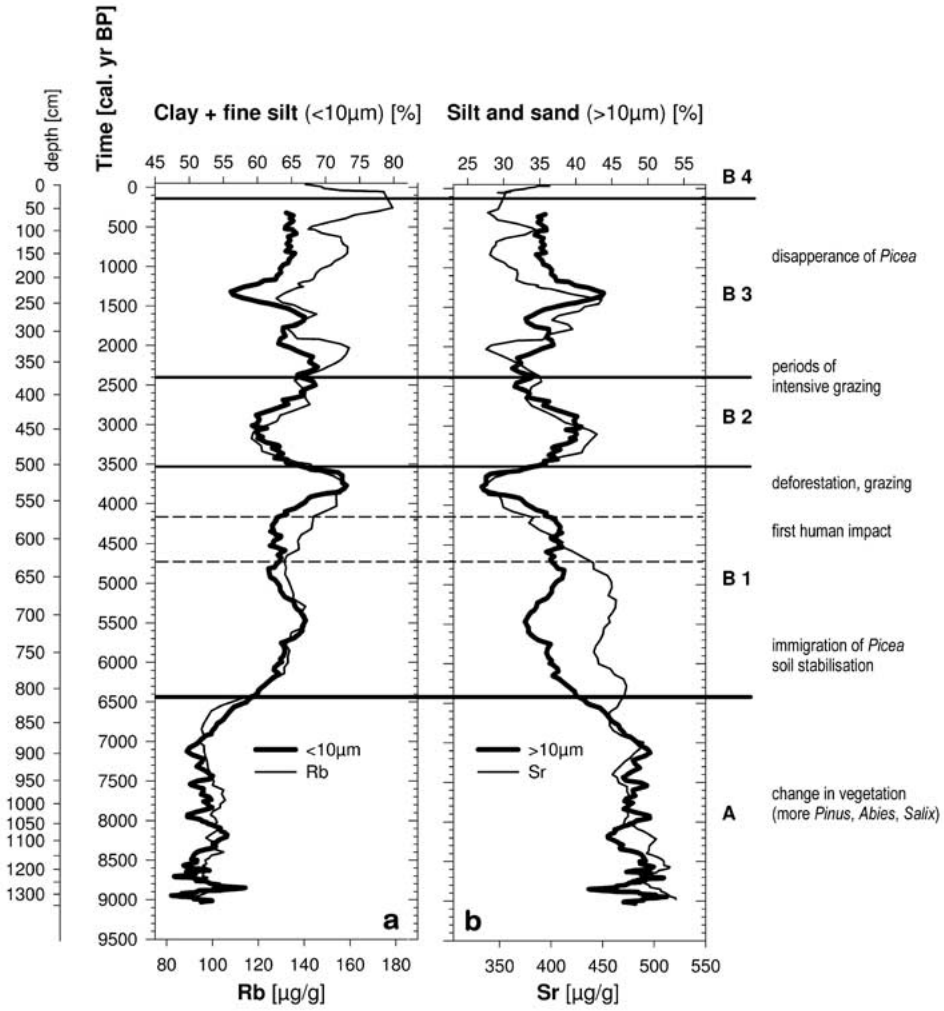

Fig. 6. Comparison of (a) rubidium concentrations vs. percent clay + fine silt (< 10 µm), and (b) strontium concentrations versus percent coarse silt + sand (> 10 µm) in the sediment of Sägistalsee. Major processes affecting grain-size and geochemistry are mentioned in the right margin. All concentrations are depicted as running means (n = 5). As both the clay (> 1–2 µm) and the fine silt fraction (2–10 µm) follow the same trend in these samples, they are depicted together.

Trace-metals (Pb, As, Zn)

From the oldest to the youngest parts of the core, concentrations of Pb, As, Zn (Fig. 3) and Ni, Cr, and Cu (data not shown) gradually increase in a comparable manner to changes in trace elements of the silicate fraction (Zr, Rb, Ti; Fig. 1). Investigating enrichment factors (EF), Pb and As (Figs 3a and 3b) depict a high variability. Arsenic only shows a very small increase in the topmost layers (EF 1.2) that cannot be separated from the long-term natural variation. In contrast, Pb shows a more distinct increase over the last 350 years when enrichment factors range between 1.2–2.4. The strongest Pb enrichment is observed in the 1970s. In the very top (last 15 years), Pb enrichment shows a slight depletion but remains elevated (Fig. 3a). Ni and Cu show no enrichment. Zn (Fig. 3c) is slightly enriched over the last 300 years (EF ca. 1.4).

Discussion

The high fluctuations observed in both the major and trace elements are closely related to variations in mineralogy and in the grain-size distribution. Deviating trends are observed in parameters often considered as indicators of redox changes (Mn and Mn/Fe, Fig. 2c). What are the processes causing these variations and what are their driving forces?

Weathering of carbonates

A gradual decrease was observed in the Ca and Sr concentrations. The major source for these elements is carbonate weathering in the catchment and in-lake precipitation of $CaCO_3$ with co-precipitation of $SrCO_3$. Consequently depletion could either be caused by a decrease in (1) physical or (2) chemical carbonate weathering, or (3) dilution by elevated silicate weathering in the catchment, or (4) pH changes in the lake, or (5) a combination of these processes. During physical weathering, $CaCO_3$ grains will be transported to the lake and, at high pH, most of the calcite grains should quickly reach the sediment without significant in-lake chemical reaction. An increase in chemical carbonate weathering will increase $CaCO_3$ dissolution and thus elevate Ca^{2+} and CO_3^{2-} transport to the lake. Given a high pH (present pH 8.4), only small amounts of Ca^{2+} remain in solution in the lake water and an increase in Ca^{2+} input will result in $CaCO_3$ precipitation. However, although the chemical composition of the lake water of Sägistalsee indicates that authigenic $CaCO_3$ precipitation is possible, Ohlendorf et al. (2003) did not observe authigenic calcite grains in 10 selected samples and the contribution of in-lake precipitation is negligible compared to detrital calcite input. In addition, Sr and Ca trends closely follow changes in grain-size (Figs. 4 and 6b) indicating that a change in physical weathering in the catchment was the major driving force for decreases in Ca and Sr concentrations in the sediment.

The transition from zone A to B, i.e., from a Ca- and Sr-rich sediment with a high proportion of coarse particles to a sediment that is relatively poor in Ca and Sr with over 50% fine particles (Figs. 1a and 6), therefore reflects a reduction in detrital carbonate input which is in agreement with the trends observed by Ohlendorf et al. (2003). In section A, when the woodland was still fairly open (see Wick et al., 2003), Ca and Sr concentrations are highest and the grain-size composition is most coarse. Ca and Sr concentrations start to decrease slightly with the immigration of *Abies alba* (around 8500 cal. BP) but the decrease is most pronounced after the immigration of *Picea abies* into the catchment area around 6500–6000 cal. BP (compare Fig. 1a, section B1). The gradual immigration of trees most certainly resulted in soil stabilisation and subsequently lower physical weathering. This argument is supported by sediment accumulation rates, which start to decrease in section A and are lowest and remain very stable in zone B1 which represents the period with the densest woodland in the catchment. Since the onset of alpine farming (deforestation around 3700 cal. BP, see Wick et al., 2003), Sr and Ca concentrations increase again and start to fluctuate, suggesting soil instability.

Weathering of silicates

The elements originating mainly from silicates (in this study K, Rb, Ti,) and also Zr, and quartz show a constant increase, especially in zone B (Figs. 1b, 1c and 5a), and generally oppose the trends seen in Ca, Sr, and $calcite_{XRD}$. While calcite can either be of detrital or authigenic origin, quartz grains are exclusively allogenic and mainly reflect changes in physical weathering and transport. The shift to higher concentrations of Rb, K, Ti, Zr, and quartz in the sediment points to enhanced physical weathering of silicates in the watershed. This is in agreement with the observed increase in the clay and fine silt fraction (Fig. 6a) as weathered silicates are usually observed in the silt and clay fraction. However, as indicated by the decrease of carbonates, sediment accumulation rate, and coarser particles, physical weathering is actually gradually reduced in the catchment. The higher proportion of silicates observed in the sediment is thus largely a result of the reduced input of physically weathered carbonates.

The trends of Rb, Ti, and Zr closely follow changes in mineralogy and grain-size (Figs. 4, 5a and 6a). Corresponding to the changes observed in carbonates, major shifts in the silicate fraction, in grain-size, and in quartz are concurrent with vegetation changes in the catchment (Fig. 6). The zones, which have been delimited independently for both the geochemistry and plant macrofossil (Wick et al., 2003) data sets match well, especially the boundaries around 6500 cal. BP (period of immigration of *Picea* resulting in soil stabilisation, the lowest sediment accumulation rates, and a high proportion of the silicate fraction) and around 3700–3500 cal. BP (onset of deforestation causing soil destabilisation and pronounced fluctuations in the silicate

fraction). This suggests that catchment vegetation was also the controlling factor for changes in silicate weathering.

Establishment of anoxia and changes in manganese and iron

Since ca. 4700 cal. BP, Mn concentrations start to vary independently of the trends observed in Fe and in the silicate fraction. In contrast, they follow the trends of $C_{inorg.}$ or calcite and contrast with those of $C_{org.}$. How can the decoupling of Mn variations from that of Fe and the silicate fraction be explained? There are a number of lines of evidence to suggest that in Sägistalsee it was the redox potential (pε) that controlled Mn concentrations since ca. 4700 cal. BP:

(1) Low concentrations of Mn coincide with low Mn/Fe ratios and high $C_{org.}$ concentrations. The Mn/Fe ratio is commonly used as indicator for palaeo-redox conditions (Wersin et al., 1991; Davison, 1993; Stumm and Morgan, 1996): Generally the reduced form of Fe is less stable in the water column than that of Mn and consequently Mn/Fe ratios in the sediment are low when the sediment becomes anoxic. At low pε, the mobilised, reduced from of iron, Fe^{2+}, re-precipitates as $FeCO_3$, or, more commonly, as FeS_2. In contrast, Mn^{2+} mainly precipitates as $MnCO_3$ and is therefore also more dependent on pH. In Sägistalsee, $MnCO_3$ will precipitate at high pH and low pε (cf. Dean, 1999; Stevens et al., 2000). However, the periodically higher $C_{org.}$ concentrations in the sediment cause higher decomposition rates. Consequently the consumption of oxygen is increasing while pH is decreasing due to the release of CO_2 into the unmixed bottom-water layer. When pH is decreasing, $MnCO_3$ becomes less stable and more manganese is mobilised - thus depleting the Mn/Fe ratio. In addition, the pH changes will affect authigenic $CaCO_3$ precipitation. However, in Sägistalsee the authigenic $CaCO_3$ precipitation is masked by the high amounts of detrital $CaCO_3$ input (see carbonate weathering). Still, since ca. 4700 cal. BP, periods of low Mn/Fe-ratios are concurrent with periods of high $C_{org.}$ concentrations (Fig. 2c). Degradation of organic matter in the bottom water must have caused oxygen depletion and low pH during these more productive periods. Consequently, larger amounts of Mn^{2+} remained in solution.

(2) In addition, only very low numbers of chironomid head capsules are observed in the sediment during periods of low Mn/Fe ratios (Heiri and Lotter, 2003). Chironomids are well established indicators of changes in redox conditions (e.g., Quinlan et al., 1998; Francis, 2001; Quinlan and Smol, 2001). The concurrence of low chironomid accumulation rates with low Mn/Fe ratios and high $C_{org.}$ concentrations thus suggests further that the bottom water became periodically anoxic.

(3) During the same periods, concentrations of charcoal and non-aboreal pollen (herbs) were high indicating more intense human activity (Heiri and Lotter, 2003; Wick et al., 2003) which most likely occurred during warm phases in this alpine catchment. Warmer temperatures would have favoured lake stratification and thus promoted anoxia. Prolonged ice-free periods with higher primary productivity and enhanced topsoil erosion (related to human activities) probably has caused the higher $C_{org.}$ concentrations observed during these periods. In addition lake depth was less than in the previous sections (ca. 7 m less) due to the high sediment accumulation. The pε of the shallower bottom water might have been more sensitive to increases in the decomposition rate caused by the higher $C_{org.}$ concentration.

(4) Further evidence is given by the mineral magnetic record, which also points to the occurrence of low redox conditions during periods of low Mn/Fe (Hirt et al., 2003).

However, the establishment of anoxia was a gradual process. In zone A and section B1, the lake became more productive (Fig. 2c). At the same time the increasing proportion of the silicate fraction resulted in higher concentrations of Mn and Fe (Figs. 2a and 2b). After a transition period in the lower part of B1, Mn and Mn/Fe started to follow $C_{inorg.}$ thus likely indicating the onset of authigenic $MnCO_3$ precipitation with a strong dependency on pH and pε. Since 4700 cal. BP, high $C_{org.}$ corresponds to low Mn, Mn/Fe, and $C_{inorg.}$ (Figs. 2b and 2c). The variations of the Mn/Fe ratios in sections B2 and B3 indicate that redox potential depleted periodically.

Natural changes in trace-metal concentrations and consequences for investigation of early metal pollution

Natural changes in metal concentrations in the sediment of Sägistalsee are high. A distinct difference between early, mid and late Holocene concentrations is observed (Fig. 3). Consequently the normalized values and enrichment factors also depict natural variability. The changes are correlated to variations in grain-size and mineralogy and are largely caused by climate-driven

changes in vegetation (see Wick et al., 2003; leading to soil stabilization) and weathering (enhancing erosion and dust transport). Early human impact by alpine farming caused a slight increase in metals due to higher erosion after deforestation and the onset of agriculture. During the past 350 years, Pb, As, and Zn increased to higher levels (Fig. 3). However, while the enrichment of Zn, As (Fig. 3), and also Cu and Ni, are comparable to that of Fe (Fig. 2), Ti, or Rb (Fig. 1), indicating that the increases are mainly caused by lithological changes, the stronger Pb enrichment can only be explained by elevated atmospheric pollution.

Compared to Pb enrichment in a Swiss peat-bog profile (Shotyk, 1996; Shotyk et al., 1998), anthropogenic Pb enrichment in Sägistalsee is only distinct in the top core sections (Fig. 3a). While the profile of the ombrotrophic peat bog exclusively reflects changes in atmospheric metal deposition, the profile in the lake sediment is largely dependent upon changes in the catchment (erosion, weathering). In the sediment of Sägistalsee, the Pb background concentrations and the range of natural variations are high. As a consequence, early atmospheric metal pollution (e.g., the Roman or Medieval lead peaks) is masked by high background concentrations and high natural variability. Metal enrichment is only detected in the past centuries due to increased pollution resulting from industrialization and leaded gasoline.

The influence of changes in vegetation, climate and human activities

As discussed in detail for carbonate and silicate weathering, several catchment and in-lake processes affected the geochemical stratigraphies (Table 2) among which changes in catchment vegetation (described by Wick et al., 2003) had the most pronounced influence. Warming after the late-glacial period led to a gradual immigration of trees (*Pinus cembra, Abies alba*). After *Picea* immigrated around 6500–6000 cal. BP, the slopes became covered with denser woodland and were subsequently less sensitive to weathering. As a consequence, the sediment accumulation rate and the supply of coarser particles, dominated by $CaCO_3$ in Sägistalsee, decreased (Figs. 1a, 6b and 7b). Both trends indicate that the denser vegetation promoted soil stabilisation. In contrast, the input of silicate minerals from the flatter basins as well as Pb, As, Zn, Ni, Cr, and Cu, increased

Table 2. Zonation of geochemical stratigraphies in Sägistalsee and related changes in the lake, in its catchment and in atmospheric pollution

Zone	Time◆	Changes in geochemistry	Changes in the lake	Changes outside the lake (catchment and atmosphere)
	1996 AD			
B4		Pb enrichment		atm. Pb pollution
	160 BP			
B3		Rb, Ti, Zr, Fe, Pb ↑↑ changes in Mn/Fe with changes in C_{inorg}	*in B2 and B3*: changes in C_{org}	*in B2 and B3*: alpine farming
	2410 BP			
B2		strong fluctuations of all elements changes in Mn/Fe with changes in C_{inorg}	changes in pH and redox changes in chironomid acc.	soil destabilisation – erosion ↑ deforestation
	3540 BP			
B1		carbonate fraction ↓↓ silicate fraction ↑	C_{org} ↑ in top: establishment of anoxic bottom water lowest sediment accumulation	immigration of *Picea* soil stabilisation – erosion ↓
	6440 BP			
A		carbonate fraction ↓	detrital calcite high sediment accumulation	immigration of *Abies* & *Pinus* more open landscape instable soils physical weathering high
	9000 BP			

◆cal. ^{14}C years BP (relative to 1950). For changes in chironomids see Heiri and Lotter (2003); for changes in vegetation see Wick et al. (2003)

(Figs. 1b, 1c, 2, 3, 5a and 6a). Later, after the onset of alpine farming, erosion increased again due to the more open landscape.

Human activities in the catchment area are traced back to ca. 4300 cal. BP, but became most pronounced around 3700–3500 cal. BP when changes in pollen and plant macrofossils indicate the onset of deforestation, grazing, and agriculture (Wick et al., 2003). At the same time, major changes in all lithogenic major and trace elements are observed (boundary between zone B1 and B2). Deforestation and grazing likely caused an increase in erosion and physical weathering and led to high variations in silt and clay, and in consequence, in all geochemical elements. Periods of more intense alpine land-use are related to high $C_{org.}$ concentrations in the sediments, pointing either to top soil erosion or higher within-lake productivity, and led to anoxic bottom water. This strongly affected the concentrations of pε- and pH-sensitive elements (Fig. 3, esp. sections B2, B3).

In contrast, the impact of climate is much more difficult to detect as it is mainly indirectly influencing sediment geochemistry. In zone A and section B1, the effect of climate on sediment geochemistry is masked by concurrent changes in the vegetation cover and by gradual soil development. In sections B2 and B3 warm periods might have promoted higher productivity and caused stronger stratification of the lake. However, the intensity of alpine farming varied at the same time and it is impossible to judge whether warming alone would have been sufficient to cause anoxic periods.

Conclusions

The sediment geochemistry of Sägistalsee is characterized by a high natural variability of all elements. Changes in catchment vegetation strongly affected the proportion of the carbonate versus the silicate fraction in the sediment with forest development reducing the losses of coarse-grained soil fractions. The onset of human impact was clearly indicated by changes in all elements. Deforestation (ca. 3700 cal. BP) caused the strongest variations in sediment geochemistry due to the destabilisation of soils. Redox-sensitive elements reflected variations in $C_{org.}$ and indicated phases with anoxia that were related to periods of intensified alpine land-use. Climate impact overlapped with the influence of vegetational changes and is difficult to separate from the effect of human activities. Due to high background concentrations and strong variations in metal concentrations, anthropogenic Pb enrichment is observed only in the topmost layers. In Sägistalsee, bulk geochemistry has proved to be a sensitive indicator of both changes in the lake and in its catchment. Its potential to provide information about palaeoenvironmental conditions should be utilized more often in palaeolimnological studies.

Acknowledgement

We owe special thanks to Andriy Cheburkin and Helen Kurzel for help during analyses of the samples with EMMA-XRFA and for their hospitality. We are grateful to all the people involved in the investigation of samples from Sägistalsee for helpful discussions and for giving us access to their data, especially Oliver Heiri, Ann Hirt, Luca Lanci, and Lucia Wick; and to S. Andreatta, M.R. Talbot, and J.F. Boyle for comments on the manuscript. Funding for sampling was provided within the framework of the European Union Environment and Climate project 'CHILL-10,000' (Climate history as recorded by ecologically sensitive arctic and alpine lakes during the last 10,000 years: a multi-proxy approach; contract No. ENV4-CT97-0642) and by the Swiss National Science Foundation within the framework of Priority Programme Environment (project 5001-044600). K. Koinig was funded by an Erwin-Schrödinger-fellowship from the Austrian Science Foundation, projects No. J-1788 Geo and J-1963 Geo. This is CHILL Contribution 40.

References

Bennett K.D. 1996. Determination of the number of zones in a biostratigraphical sequence. New Phytol. 132: 155–170.

Blais J.M. and Kalff J. 1993. Atmospheric loading of Zn, Cu, Ni, Cr, and Pb to lake-sediments – the role of catchment, lake morphometry, and physicochemical properties of the elements. Biogeochemistry 23: 1–22.

Boyle J.F. 2000. Rapid elemental analysis of sediment samples by isotope source XRF. J. Paleolim. 23: 213–221.

Brännvall M.L., Bindler R., Emteryd O. and Renberg I. 2001. Four thousand years of atmospheric lead pollution in Northern Europe: a summary from Swedish lake sediments. J. Paleolim. 25: 421–435.

Brännvall M.L., Bindler R., Renberg I., Emteryd O., Bartnicki J. and Billstrom K. 1999. The Medieval metal industry was the cradle of modern large scale atmospheric lead pollution in northern Europe. Envir. Sci. Technol. 33: 4391–4395.

Brenner M., Whitmore T.J., Curtis J.H., Hodell D.A. and Schelske C.L. 1999. Stable isotope (delta C-13 and delta N-15) signatures of sedimented organic matter as indicators of historic lake trophic state. J. Paleolim. 22: 205–221.

Camarero L., Masque P., Devos W., Ani Ragolta I., Catalan J., Moor H.C., Pla S. and Sanchez Cabeza J.A. 1998. Historical variations in lead fluxes in the Pyrenees (northeast Spain) from a dated lake sediment core. Wat. Air. Soil Pollut. 105: 439–449.

Cheburkin A.K., Frei R. and Shotyk W. 1997. An Energy-Dispersive Miniprobe Multielement Analyzer (EMMA) for direct analysis of trace-elements and chemical age dating of single mineral grains. Chem. Geol. 135: 75–87.

Cheburkin A.K. and Shotyk W. 1996. An Energy-Dispersive Miniprobe Multielement Analyzer (EMMA) for direct analysis of Pb and other trace-elements in peats. Fresenius. J. Anal. Chem. 354: 688–691.

Davison W. 1993. Iron and manganese in lakes. Earth Sci. Rev. 34: 119–163.

Dean W.E. 1999. The carbon cycle and biogeochemical dynamics in lake sediments. J. Paleolim. 21: 375–393.

Engstrom D.R., Swain E.B. and Kingston J.C. 1985. A palaeolimnological record of human disturbance from Harvey's Lake, Vermont: geochemistry, pigments and diatoms. Freshwat. Biol. 15: 261–288.

Francis D.R. 2001. A record of hypolimnetic oxygen conditions in a temperate multi-depression lake from chemical evidence and Chironomid remains. J. Paleolim. 25: 351–365.

Heiri O. and Lotter A.F. 2003. 9000 years of chironomid assemblage dynamics in an Alpine lake: long-term trends, sensitivity to disturbance of resilience of the fauna. J. Paleolim. 30: 273–289.

Hirt A.M., Lanci L. and Koinig K.A. 2003. Mineral magnetic record of Holocene environmental changes in Sägistalsee, Switzerland. J. Paleolim. 30: 321–331

Hofmann W. 2003. The long-term succession of high-altitude cladoceran assemblages: a 9000 year record from Sägistalsee (Swiss Alps, 1935 m asl). J. Paleolim. 30: 291–296

Kauppila T. and Salonen V.-P. 1997. The effect of Holocene treeline fluctuations on the sediment chemistry of Lake Kilpisjärvi, Finland. J. Paleolim. 18: 145–163.

Lamb H.F., Roberts N., Leng M., Barker P., Benkaddour A. and Van Der Kaars S. 1999. Lake evolution in a semi-arid mountain environment: Response to catchment change and hydroclimatic variation. J. Paleolim. 21: 325–343.

Legendre P. and Legendre L. 1998. Numerical Ecology. Elsevier, Amsterdam, 853 pp.

Lotter A.F. 2001. The palaeolimnology of Soppensee (Central Switzerland), as evidenced by diatom, pollen, and fossil-pigment analyses. J. Paleolim. 25: 65–79.

Lotter A.F. and Birks H.J.B. 2003. Holocene sediments of Sägistalsee, a small lake at present-day tree-line in the Swiss Alps. J. Paleolim. 30: 253–260

Norton S.A., Bienert R.W., Bienford M.W. and Kahl J.S. 1992. Stratigraphy of total metals in PIRLA sediment cores. J. Paleolim. 7: 191–214.

Norton S.A. and Kahl J.S. 1991. Progress in understanding the chemical stratigraphy of metals in lake-sediments in relation to acidic precipitation. Hydrobiologia 214: 77–84.

Ohlendorf C., Sturm M. and Hausmann S. 2003. Natural environmental changes and human impact reflected in sediments of a high alpine lake in Switzerland. J. Paleolim. 30: 297–306

Quinlan R. and Smol J.P. 2001. Setting minimum head capsule abundance and taxa deletion criteria in chironomid-based inference models. J. Paleolim. 26: 327–342.

Quinlan R., Smol J.P. and Hall R.I. 1998. Quantitative inferences of past hypolimnetic anoxia in south-central Ontario lakes using fossil midges (Diptera: Chironomidae). Can. J. Fish. aquat. Sci. 55: 587–596.

Renberg I., Wik-Persson M. and Emteryd O. 1994. Pre-industrial atmospheric lead contamination detected in Swedish lake sediments. Nature 368: 323–326.

Schwalb A., Burns S.J. and Kelts K. 1999. Holocene environments from stable isotope stratigraphy of ostracods and authigenic carbonate in Chilean Altiplano lakes. Palaeogeo. Palaeoclim. Palaeoecol. 148: 153–168.

Shotyk W. 1996. Peat bog archives of atmospheric metal deposition: geochemical evaluation of peat profiles, natural variations in metal concentrations, and metal enrichment factors. Environmental Rev. 4: 149–183.

Shotyk W., Weiss D., Appleby P.G., Cheburkin A.K., Frei R., Gloor M., Kramers J.D., Reese S. and Van der Knaap W.O. 1998. History of atmospheric lead deposition since 12,370 C-14 yr BP from a peat bog, Jura Mountains, Switzerland. Science 281: 1635–1640.

Sommaruga-Wögrath S., Koinig K.A., Schmidt R., Sommaruga R., Tessadri R. and Psenner R. 1997. Temperature effects on the acidity of remote alpine lakes. Nature 387: 64–67.

Stevens L.R., Ito E. and Olson D.E.L. 2000. Relationship of Mn-carbonates in varved lake sediments to catchment vegetation in Big Watab Lake, MN, USA. J. Paleolim. 24: 199–211.

Stumm W. and Morgan J.J. 1996. Aquatic Chemistry. Chemical Equilibria and Rates in Natural Waters. Wiley and Sons, New York, 1022 pp.

ter Braak C.J.F. and Smilauer P. 1998. CANOCO reference manual and user's guide to Canoco for Windows: Software for Canonical Community Ordination (version 4). Microcomputer Power, Ithaca, NY, USA, 352 pp.

Teranes J.L., Mckenzie J.A., Bernasconi S.M., Lotter A.F. and Sturm M. 1999. A study of oxygen isotopic fractionation during bio-induced calcite precipitation in eutrophic Baldeggersee, Switzerland. Geochim. Cosmochim. Acta 63: 1981–1989.

Valero-Garces B.L., Laird K.R., Fritz S.C., Kelts K., Ito E. and Grimm E.C. 1997. Holocene climate in the Northern Great Plains inferred from sediment stratigraphy, stable isotopes, carbonate geochemistry, diatoms, and pollen at Moon Lake, North Dakota. Quat. Res. 48: 359–369.

Wersin P., Hohener P., Giovanoli R. and Stumm W. 1991. Early diagenetic influences on iron transformations in a fresh-water lake sediment. Chem. Geol. 90: 233–252.

Wessels M., Lenhard A., Giovanoli F. and Bollhofer A. 1995. High resolution time series of lead and zinc in sediments of Lake Constance. Aquat. Sci. 57: 291–304.

White A.F., Blum A.E., Bullen T.D., Vivit D.V., Schulz M. and Fitzpatrick J. 1999. The effect of temperature on experimental and natural chemical weathering rates of granitoid rocks. Geochim. Cosmochim. Acta 63: 3277–3291.

Wick L., van Leeuwen J.F.N., van der Knaap W.O. and Lotter A.F. 2003. Holocene vegetation development in the catchment of Sägistalsee (1935 m asl), a small lake in the Swiss Alps. J. Paleolim. 30: 261–272.

Wilmshurst J.M. 1997. The impact of human settlement on vegetation and soil stability in Hawke's Bay, New Zealand. New. Zeal. J. Bot. 35: 97–111.

Wolfe A.P. and Hartling J.W. 1997. Early Holocene trace-metal enrichment in organic lake-sediments, Baffin-Island, Arctic Canada. Arct. Alp. Res. 29: 24–31.